In-silico identification of potent inhibitors of COVID-19 main protease (M^{pro}) and Angiotensin converting enzyme 2 (ACE2) from natural products: Quercetin, Hispidulin, and Cirsimaritin exhibited better potential inhibition than Hydroxy-Chloroquine against COVID-19 main protease active site and ACE2.

Omar Sekiou [1, *], Ismail Bouziane[2], Zihad Bouslama [1], Abdelhak Djemel [1]

[1]Environmental Research Center (C.R.E), Campus, Sidi Amar, Annaba 23001; Algeria

[2]REPCO. Research Product Company (McShares). Kansas, United States of America.

[*]**Corresponding author**: **E-mail address:** sekiouomar@yahoo.fr; omar.sekiou@univ-annaba.org

Abstract

COVID-19 is rapidly spreading and there are currently no specific clinical treatments available. The absence of an immediate available vaccine against SARS-CoV-2 made it hard for health professionals to tackle the problem. Thus, the need of ready to use prescription drugs or herbal remedies is urgent. SARS-CoV-2 main protease (Mpro) and Angiotensin Converting Enzyme2 (ACE2) protein structure are made available to facilitate finding solutions to the present problem. In this brief research, we compare the efficacy of some natural compounds against COVID-19 Mpro and ACE2 to that of Hydroxy-Chloroquine *in silico*.

Molecular docking investigations were carried out using AutoDock. Virtual screening was performed using AutoDock Vina and the best ligand / protein mode was identified based on the binding energy. Amino Acids residues of ligands interactions were identified using PyMOL. According to present research results, Quercetin, Hispidulin, Cirsimaritin, Sulfasalazine, Artemisin and Curcumin exhibited better potential inhibition than Hydroxy-Chloroquine against COVID-19 main protease active site and ACE2. Our provided docking data of these compounds may help pave a way for further advanced research to the synthesis of novel drug candidate for COVID-19.

Keywords: COVID-19 main protease (M^{pro}), SARS-CoV-2, Molecular docking, Angiotensin converting enzyme2 (ACE2).

1. Introduction

Coronaviruses are a large family of enveloped, RNA viruses. There are 4 groups of coronaviruses: alpha and beta, originated from bats and rodents; and gamma and delta, originated from avian species (Su et al., 2016). Coronaviruses are responsible for a wide range of diseases in many animals, including livestock and pets (Belouzard et al., 2012). In humans, they were thought to cause mild, self-limiting respiratory infections until 2002, when a beta-coronavirus crossed species barriers from bats to a mammalian host, before jumping to humans, causing the Severe Acute Respiratory Syndrome, SARS, epidemic. More recently, another beta-coronavirus is responsible for the serious Middle East Respiratory Syndrome, MERS, started in 2012 (Mcintosh et Perlman, 2015). The novel coronavirus responsible for the Coronavirus Disease 2019 pandemic, COVID-19, is also a beta-coronavirus (Liu et al., 2020). The genome of the virus is fully sequenced and appears to be most similar to a strain in bats, suggesting that it also originated from bats. The virus is also very similar to the SARS-coronavirus and is therefore named SARS-coronavirus 2, SARS-CoV 2 (Robson et al., 2020). In order to infect a host cell, the spikes of the virus must bind to a molecule on the cell surface. The novel coronavirus appears to use the same receptor as SARS-coronavirus for entry to human cells, and that receptor is the angiotensin-converting enzyme 2, ACE2. (Liu et al.2020). Infection usually starts with cells of the respiratory mucosa, then spreads to epithelial cells of alveoli in the lungs. Receptor binding is followed by fusion of the viral membrane with host cell membrane, and the release of nucleocapsid into the cell.

Currently, no specific clinical therapies are available for the treatment of SARS-CoV-2 mediated infections (Zhou et al., 2020). Thus, the need of the hour is the identification and characterization of a new drug candidate to inhibit binding between the COVID-19 main protease (M^{pro}) and the angiotensin-converting enzyme 2, on the cell surface. To this aims, we have screened *in silico* the interaction between the main protease COVID-19 (M^{pro}) active site as well as the binding and active site of angiotensin-converting enzyme2 (ACE2) with natural compounds that displays a large variety of biological activities.

2. Experimental design, materials, and methods

Computational chemistry or as known as molecular modeling is a fascinating branch of chemistry. It uses modeling and virtual simulations to help solve chemistry modern problems. Lately, virtual screening of compound libraries has become a standard technology in modern drug discovery pipelines (Kitchen et al., 2004). In our study, to perform in-silico specific site docking, we used a powerful bioinformatics tool; AutoDock. In order to visualize the data, we utilized PyMOL software.

2.1. Protein selection and preparation

The complete genome of Angiotensin converting enzyme2 ACE2 was retrieved from PDB. PDB ID: 1r42. And The main protease of COVID-19 was retrieved from PDB. PDB ID: 6LU7

The downloaded structures were prepared prior to docking as fellow:

First, we visualized the PDB file in PyMOL then removed hetatoms and kept only Chain A. Next, we optimized hydrogen bonds structures and added atoms in missing loops or side chains. Finally, we removed water molecules and saved our files in a PDB file format.

2.2. Ligand preparation

The structures of our ligands were downloaded from PubChem (https://pubchem.ncbi.nlm.nih.gov/) and saved in SDF format. Files were converted from SDF to PDB format using PyMOL.

2.3. Molecular docking

Docking sites targeted for ACE2 are; site (375,505,273,345,371,30 to 41,82 to 84, and 353 to 357). The coordinates of the position are X: 62.170 Y: 69.041, and Z: 28.353 at grid spacing of 1 Angstrom. For 6LU7 molecular docking, the selected cavity is the binding site of inhibitor N3. The coordinates of the position are X: -16.308 Y: 11.57, and Z: 72.881 at grid spacing of 0.500 Angstrom. Virtual screening was carried our using AutoDock Vina and the best ligand / protein mode was identified based on the binding energy. The scoring function of AutoDock Vina is: $C=\sum i<jftitj(rij)$, where the summation is over all of the pairs of atoms that can move relative to each other, normally excluding 1–4 interactions, i.e. atoms separated by 3 consecutive covalent bonds. Here, each atom i is assigned a type ti, and a symmetric set of interaction functions ftitj of the interatomic distance rij should be defined (Oleg et Arthur 2010).

.

3. Data

In this article: Table 1. Shows the PDB ID, resolution and description of Angiotensin converting enzyme2 ACE2 & COVID-19 main protease selected for this study. Table 2. provides the structure of chosen ligands. Table 3. gives docking results of COVID-19 main protease 6LU7. Table 4. represents docking results of ACE2. The 3D interactions of the high scored ligands with ACE2 and COVID-19 main protease active sites are shown in Figure1 -Figure14

Table 1: PDB ID, resolution and description of Angiotensin converting enzyme2 ACE2 and COVID-19 main protease.

Protein	PDB ID	Resolution (Å)	Structure
Angiotensin converting enzyme2 (ACE2)	1R42	2.20 Å	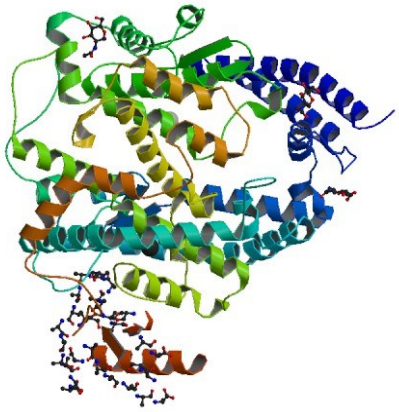
COVID-19 main protease	6LU7	2.16 Å	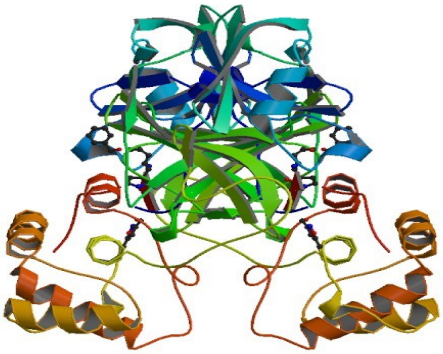

Table2: Name of ligand and structure (https://pubchem.ncbi.nlm.nih.gov)

Name of ligand	Structure of ligand	Name of ligand	Structure of ligand
Quercetin	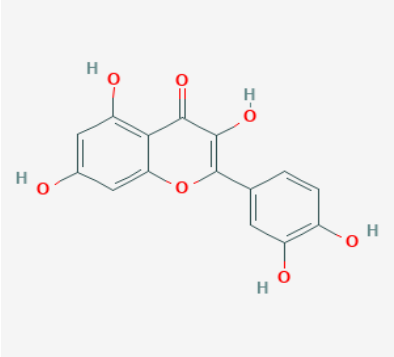	**Hispidulin**	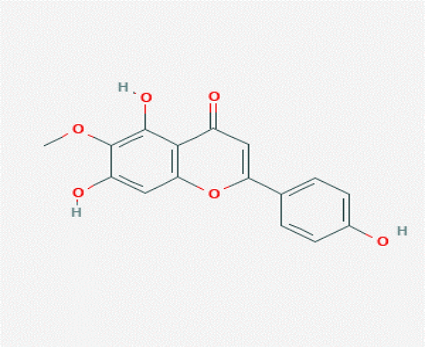
Cirsimaritin	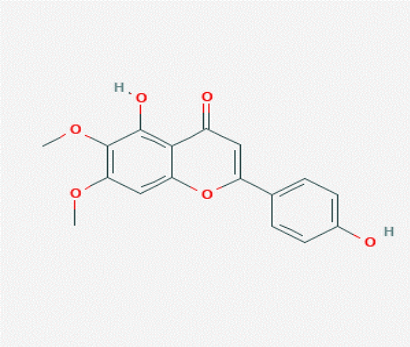	**Artemisin**	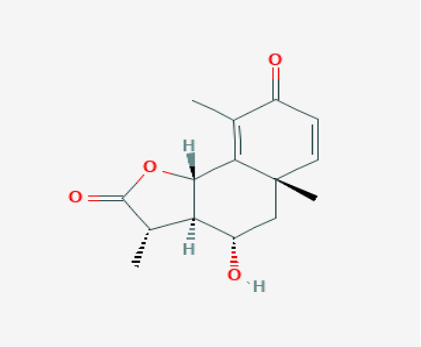
Curcumin	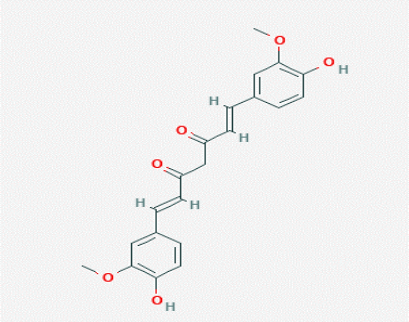	**Hydroxy-Chloroquine**	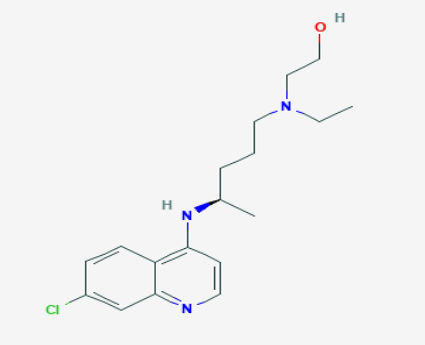
Thymoquinone	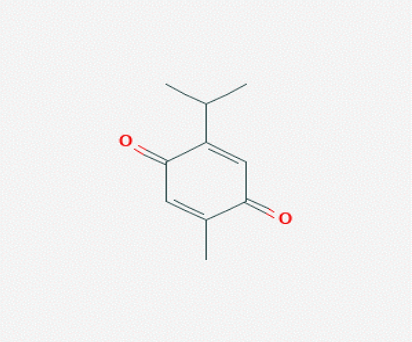	**Eugenol**	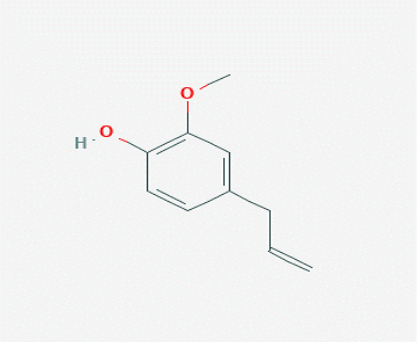

N-acetylcysteine	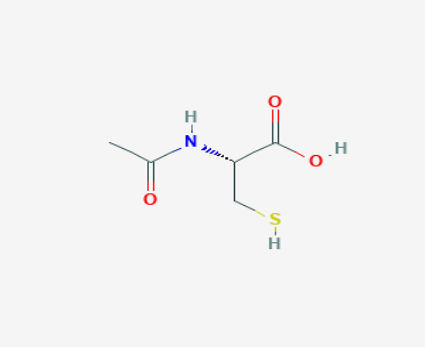	**Sulfasalazine**	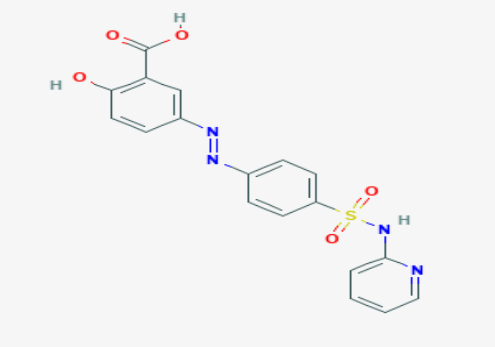

4. Results

4.1. Results of binding energies obtained from the docking (AutoDock Vina) of COVID-19 main protease (6LU7) active site.

The binding energies obtained from the docking (AutoDock Vina) of the active site of COVID-19 main protease 6LU7 were presented in Table 3.

Quercetin, Hispidulin, Cirsimaritin, Sulfasalazine, Artemisin and Curcumin showed low binding energy to 6LU7 active site than that of Hydroxy-Chloroquine (Table 3). Quercetin: exhibited the lowest binding energy to 6LU7. As shown in Table 3, Figure 1. Quercetin was well fitted into the active pocket of 6LU7 and its hydroxy groups formed hydrogen bonds with Leu141 and His163.Hispidulin: exhibited the second lowest binding energy at the active site of COVID-19 main protease Table 3. Hispidulin was well fitted into the active pocket of 6LU7 and its hydroxy groups formed hydrogen bonds with His163, Leu141, Ser144, Glu166, and Cys145, which compose a relatively hydrophobic environment Figure 2. Cirsimaritin: Predicted results illustrate that 6LU7 critical binding residue; Glu166, His163, Cys145, Leu141, and Ser144 form hydrogen bonds with Cirsimaritin (Table 3, Figure 3). Sulfasalazine: Amino acids predicted for Sulfasalazine binding in COVID-19 main protease were Gly143, Ser144, and Cys145, as shown in Table 3, Figure 4. Artemisin: Hydrogen bonding was predicted between 6LU7 actives sites His163 & Glu166 and the hydroxy functional group as shown in Table 3, Figure 5. Curcuma: Hydrogen bonding was predicted between Glu 166 and the hydroxy group of the compound (Table 3, Figure 6). Hydroxy-Chloroquine: Hydrogen bonding was predicted between Asn142, His164, and His163 and the hydroxy group of the compound (Table 3, Figure 7). Thymoquinone: Hydrogen bonding was predicted between His164 and the hydroxy group of the compound (Table 3, Figure 8). Eugenol: Hydrogen bonding was predicted to form between (Leu141, His163, Ser144, Gly143, Cys145) and the hydroxy group of the compound (Table 3).

N-acetylcysteine: Hydrogen bonding was predicted to form between (Gly143, Leu141, Ser144, Cys145, His163) and the hydroxy group of the compound (Table 3). Camphor: Hydrogen bonding was predicted to form between Glu166 and the hydroxy group of the compound (Table 3).

Table 3. The hydrogen bond energy of the Quercetin, Hispidulin, Cirsimaritin, Sulfasalazine, Artemisin, Curcuma, Hydroxy-Chloroquine, thymoquinone, Eugenol, N-acetylcysteine, and Camphor binding to the cavity M^{pro} of COVID-19. Coordinates of the docking position are X: -16.308 Y: 11.57, and Z: 72.881. Grid resolution = 0.500 Angstrom.

Compounds	Hydrogen bond Number	Length	Affinity (kcal/mol)	Predicted Amino Acids residues interaction
Quercetin	1 2	1.9 2.2	**-7.5**	His163, Leu141
Hispidulin	1 2 3 4 5	2.2 2.3 2.4 2.7 3.5	**-7.3**	His163, Leu141, Ser144, Glu166, Cys145
Cirsimaritin	1 2 3 4 5	2.2 2.3 2.3 2.4 2.6	**-7.2**	Glu166, His163, Cys145, Leu141, Ser144
Sulfasalazine	1 2 3 4	2.2 2.3 2.5 2.7	**-7.2**	Gly143, Ser144, Cys145
Artemisin	1 2	2.2 2.3	**-6.8**	His163, Glu166
Curcuma	1	2.4	**-6.8**	Glu166
Hydroxy-Chloroquine	1 2 3	2.3 2.8 3.4	**-5.9**	Asn142, His164, His163
Thymoquinone	1	3.4	**-5.1**	His164
Eugenol	1 2 3 4 5	1.8 2.1 2.2 2.6 2.7	**-4.9**	Leu141, His163, Ser144, Gly143, Cys145
N-acetylcysteine	1 2 3 4	2.0 2.0 2.1 2.3	**-4.6**	Gly143, Leu141, Ser144, Cys145, His163
Camphor	1	2.0	**-4.5**	Glu166

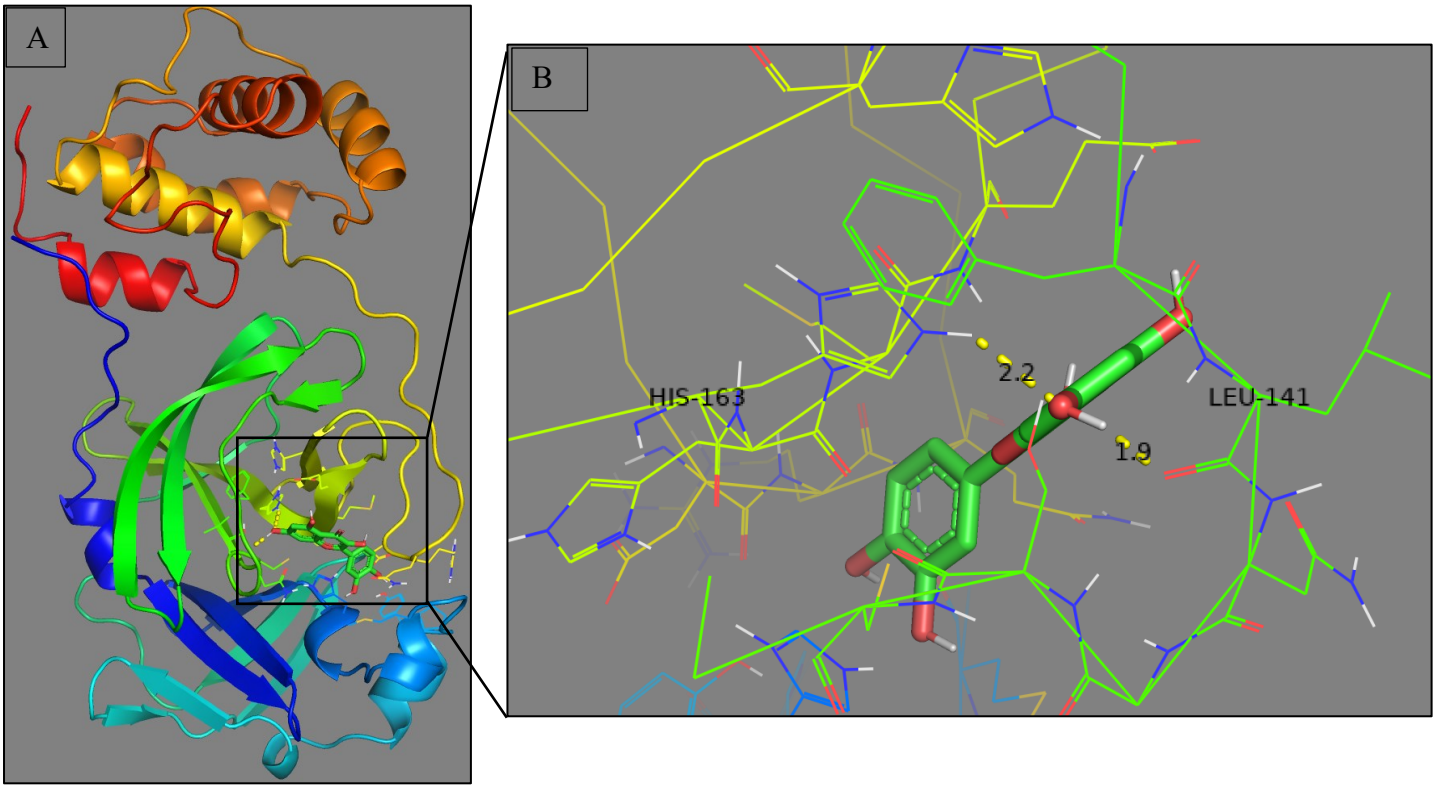

Figure 1. Representation of docked ligand-protein complex (A) animation pose of Quercetin within the cavity of 6LU7, (B) Interaction of Quercetin with amino acid residues of M^{pro} COVID-19.

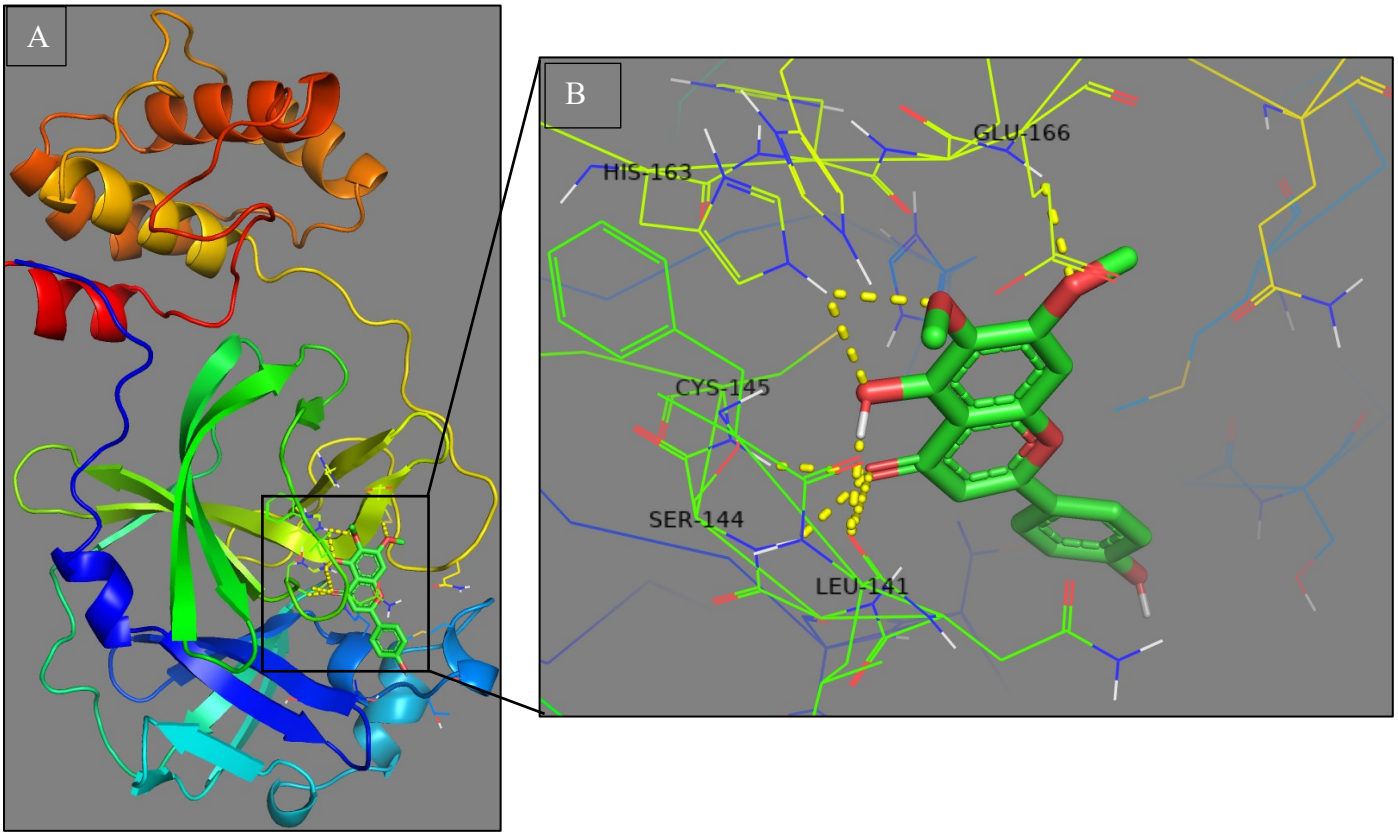

Figure 2. Representation of docked ligand-protein complex (A) animation pose of Hispidulin within the cavity of 6LU7, (B) Interaction of Hispidulin with amino acid residues of M^{pro} COVID-19.

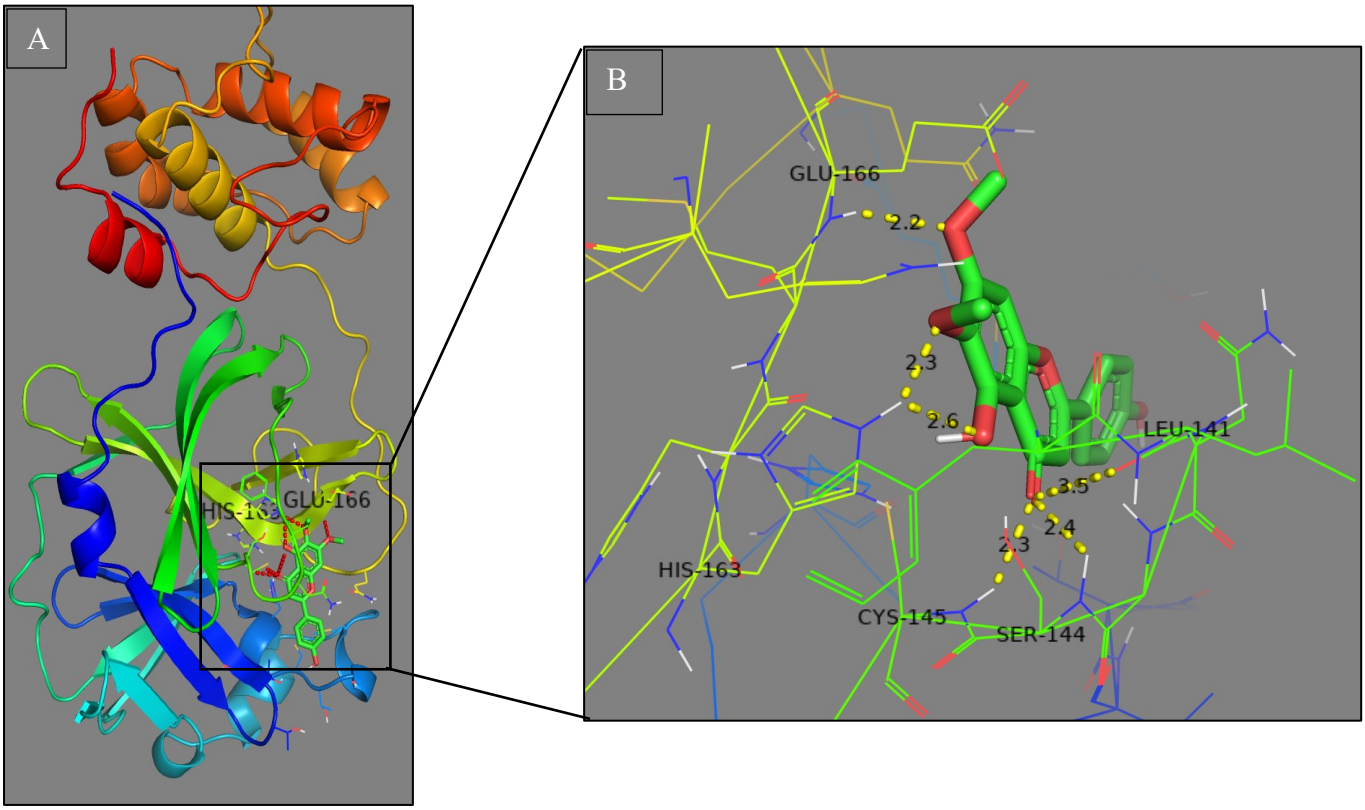

Figure 3. Representation of docked ligand-protein complex (A) animation pose of Cirsimaritin within the cavity of 6LU7, (B) Interaction of Cirsimaritin with amino acid residues of M^{pro} COVID-19.

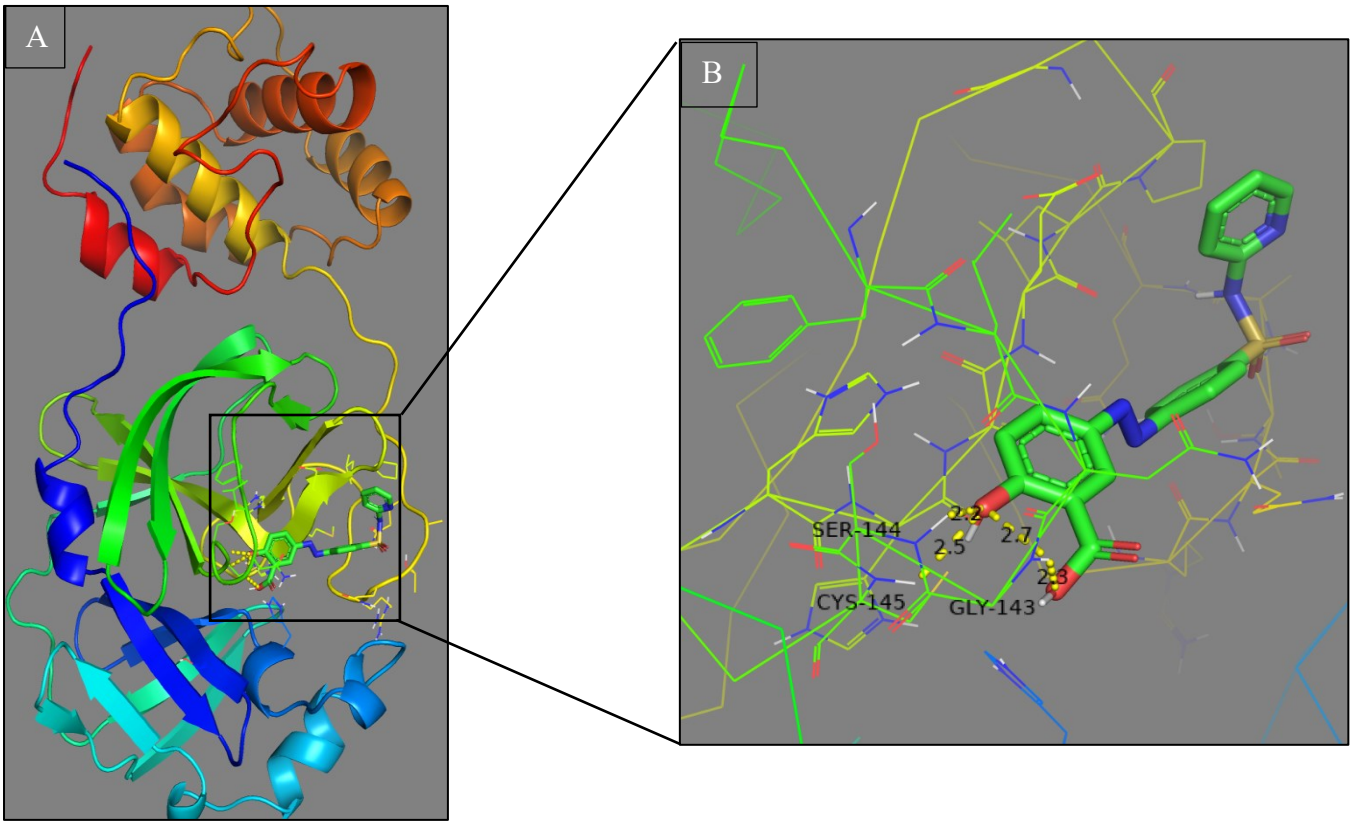

Figure 4. Representation of docked ligand-protein complex (A) animation pose of Sulfasalazine within the cavity of 6LU7, (B) Interaction of Sulfasalazine with amino acid residues of M^{pro} COVID-19.

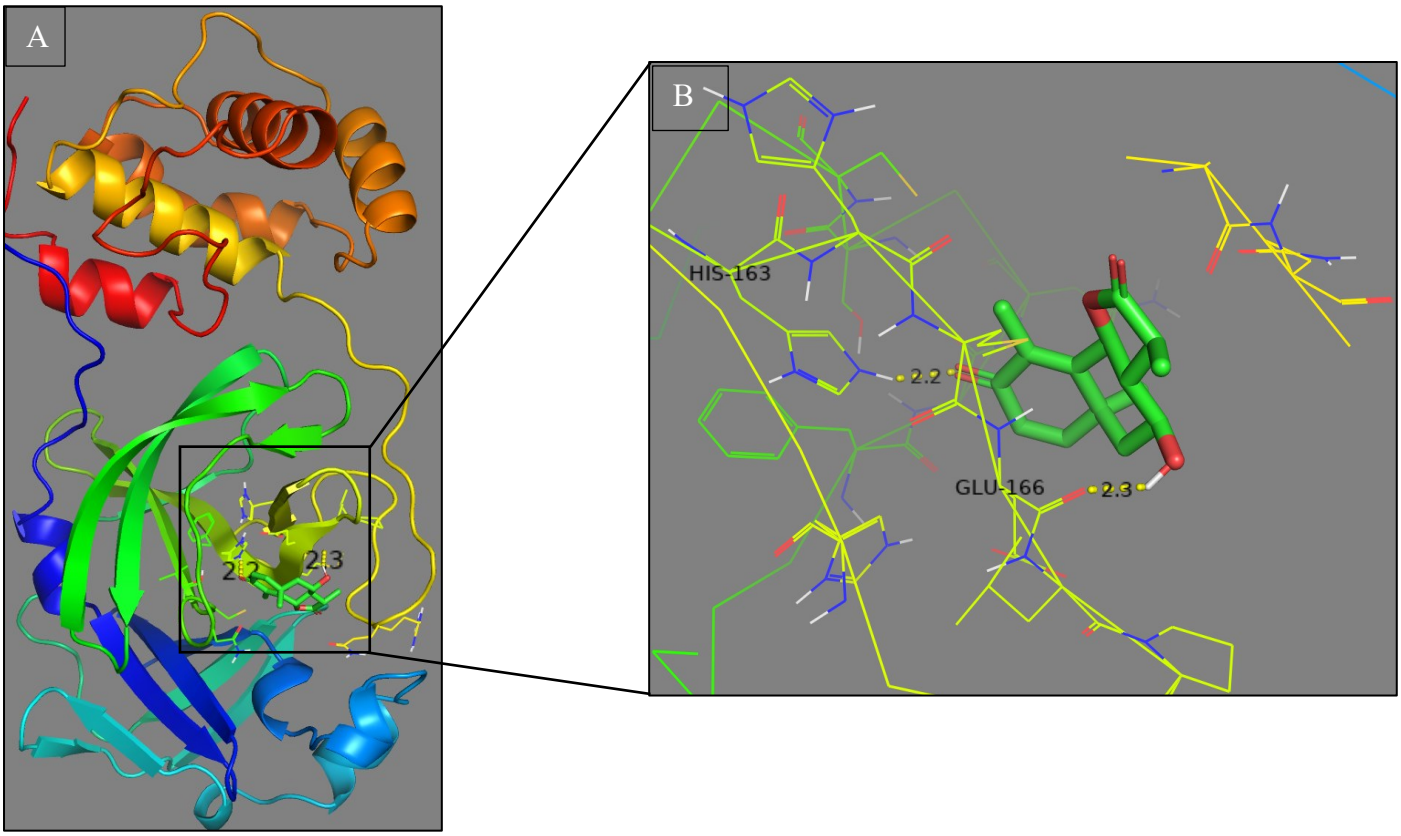

Figure 5. Representation of docked ligand-protein complex (A) animation pose of Artemisin within the cavity of 6LU7, (B) Interaction of Artemisin with amino acid residues of M^{pro} COVID-19.

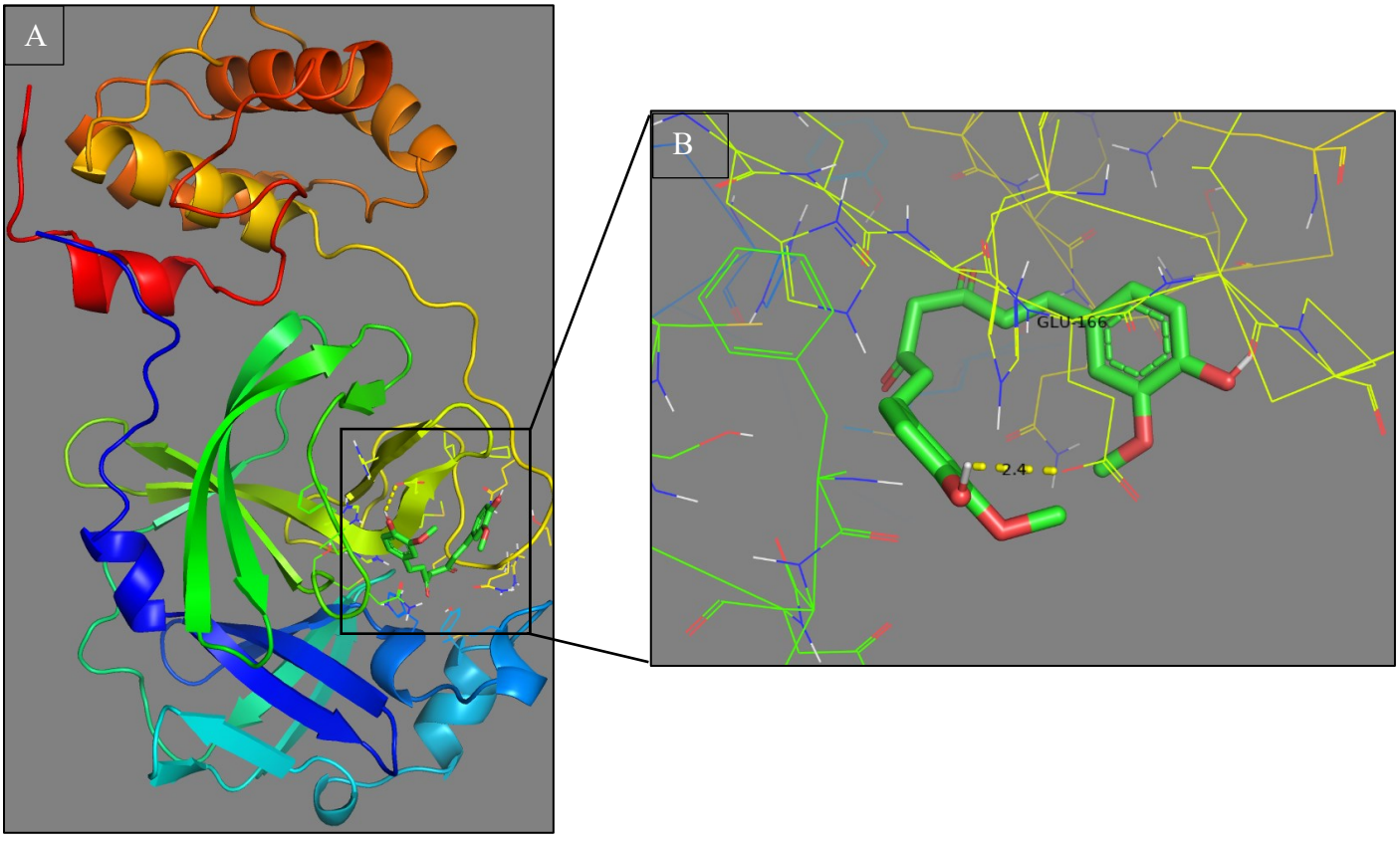

Figure 6. Representation of docked ligand-protein complex (A) animation pose of Curcuma within the cavity of 6LU7, (B) Interaction of Curcuma with amino acid residues of M^{pro} COVID-19.

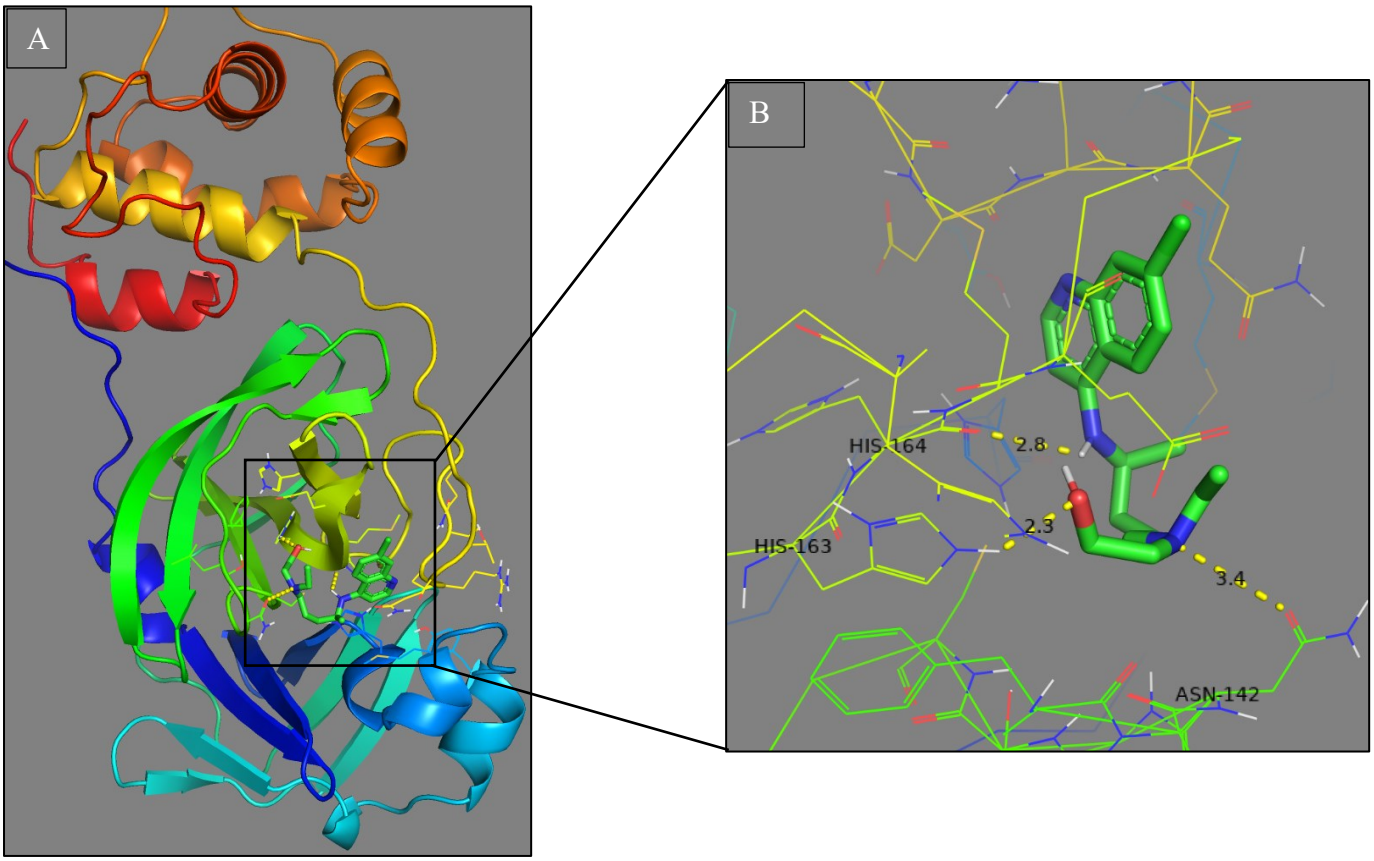

Figure 7. Representation of docked ligand-protein complex (A) animation pose of Hydroxy-Chloroquine within the cavity of 6LU7, (B) Interaction of Hydroxy-Chloroquine with amino acid residues of M^{pro} COVID-19

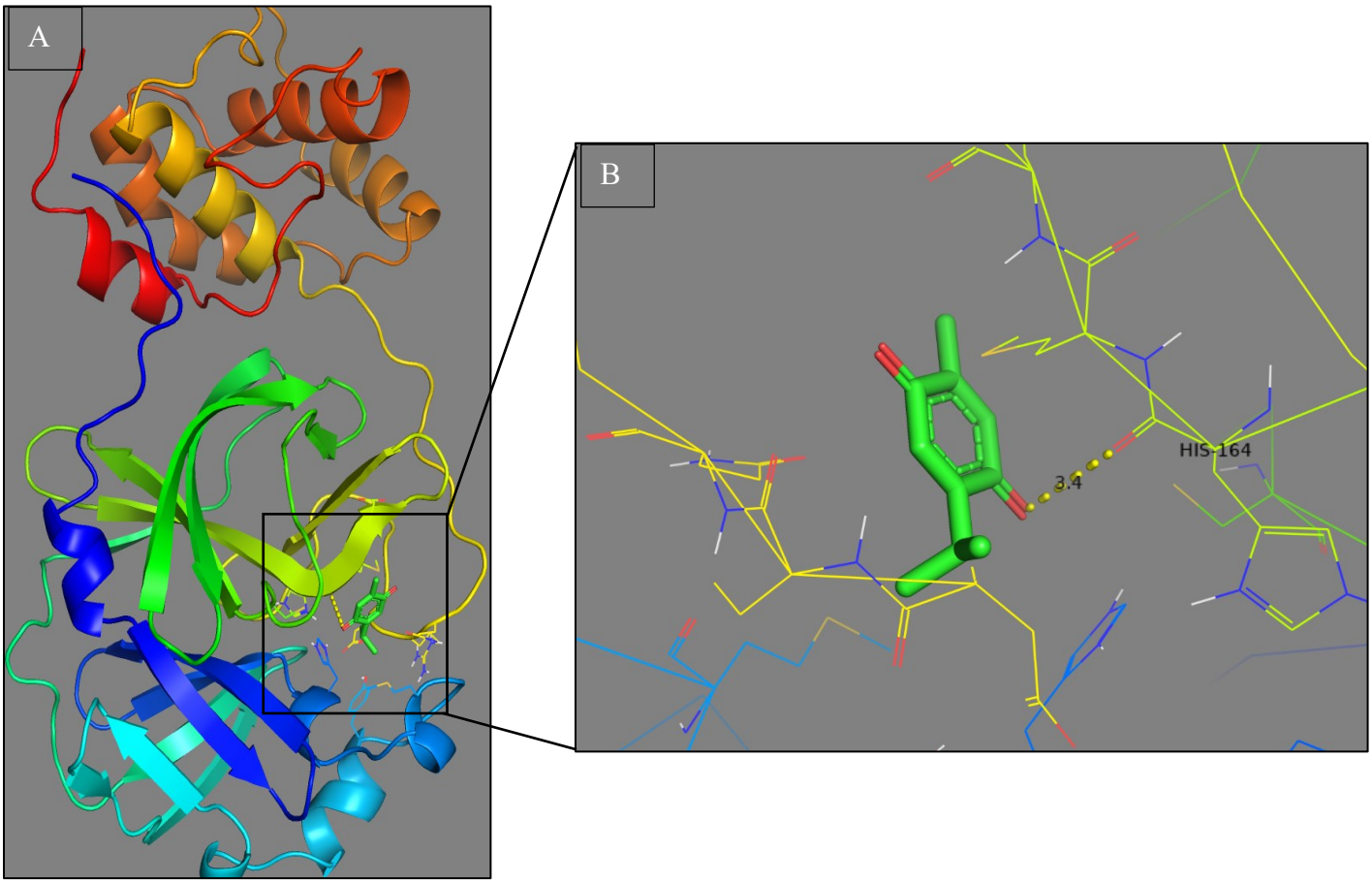

Figure 8. Representation of docked ligand-protein complex (A) animation pose of Thymoquinone within the cavity of 6LU7, (B) Interaction of Thymoquinone with amino acid residues of M^{pro} COVID-19

4.2. Results of binding energies obtained from the docking (AutoDock Vina) of ACE2 active site.

The binding energies obtained from the docking (AutoDock Vina) of the active site of ACE2 were presented in Table 4. Hispidulin, Cirsimaritin, Artemisin and Curcumin showed low binding energy to ACE2 active site than that of Hydroxy-Chloroquine (Table 4). Hispidulin exhibited the highest binding energy at the active site of ACE2 active site (Table 4, Figure 9), it formed hydrogen bond interactions with TYR196, GLY564, and TRP566. The results shown that critical residues for the binding of Cirsimaritin to ACE2 active site were TYR196, and ASP206 (Table 4, Figure 10). Amino acids responsible for Artemisin binding in ACE2 active site were TYR196, and ASN103 (Table 4, Figure 11). Curcuma participated hydrogen bond interactions with active site residues LYS94, and TRP566 of ACE2 (Table 4, Figure 12). Hydroxy-Chloroquine participated hydrogen bond interactions with TYR127, HIS505, ARG273, and GLU145 of ACE2 active site (Table 4, Figure 13). Eugenol participated hydrogen bond interactions with ASN290 of ACE2 active site (Table 4, Figure 14). Amino acids responsible for Thymoquinone binding in ACE2 is GLY-211 (Table 4). Table 4 demonstrated that TRP566 amino acids is responsible for N-acetylcysteine binding in ACE2 active site. Amino acids responsible for Camphor binding in ACE2 is TYR-196 (Table 4).

Table 4. The hydrogen bond energy of the Hispidulin, Cirsimaritin, Artemisin, Curcuma, Hydroxy-Chloroquine, Thymoquinone, Eugenol, N-acetylcysteine, and Camphor binding to ACE2. Coordinates of the docking position are X: 62.170 Y: 69.041, and Z: 28.353. Grid resolution = 1 Angstrom

Compounds	Hydrogen bond Number	Length	Affinity (kcal/mol)	Amino Acids residues interaction
Hispidulin	1 2 3 4	2.8 3.0 2.0 **3.0**	**-7.8**	TYR196, GLY564, TRP566
Cirsimaritin	1 2 3 4	**3.2** **2.3** **3.5** **3.3**	**-7.6**	TYR196, ASP206
Artemisin	1 2	2.9 3.1	**-7.2**	TYR196, ASN103
Curcuma	1 2 3	3.4 3.0 2.9	-7.2	LYS94, TRP566
Hydroxy-Chloroquine	1 2 3 4	2.5 3.0 3.3 3.1	-6.4	TYR127, HIS505, ARG273, GLU145
Eugenol	1 2	2.3 3.2	-6.3	ASN290
Thymoquinone	1	3.3	**-5.5**	GLY-211
N-acetylcysteine	1	2.8	-4.5	TRP 566
Camphor	1	2.9	**-4.8**	TYR-196

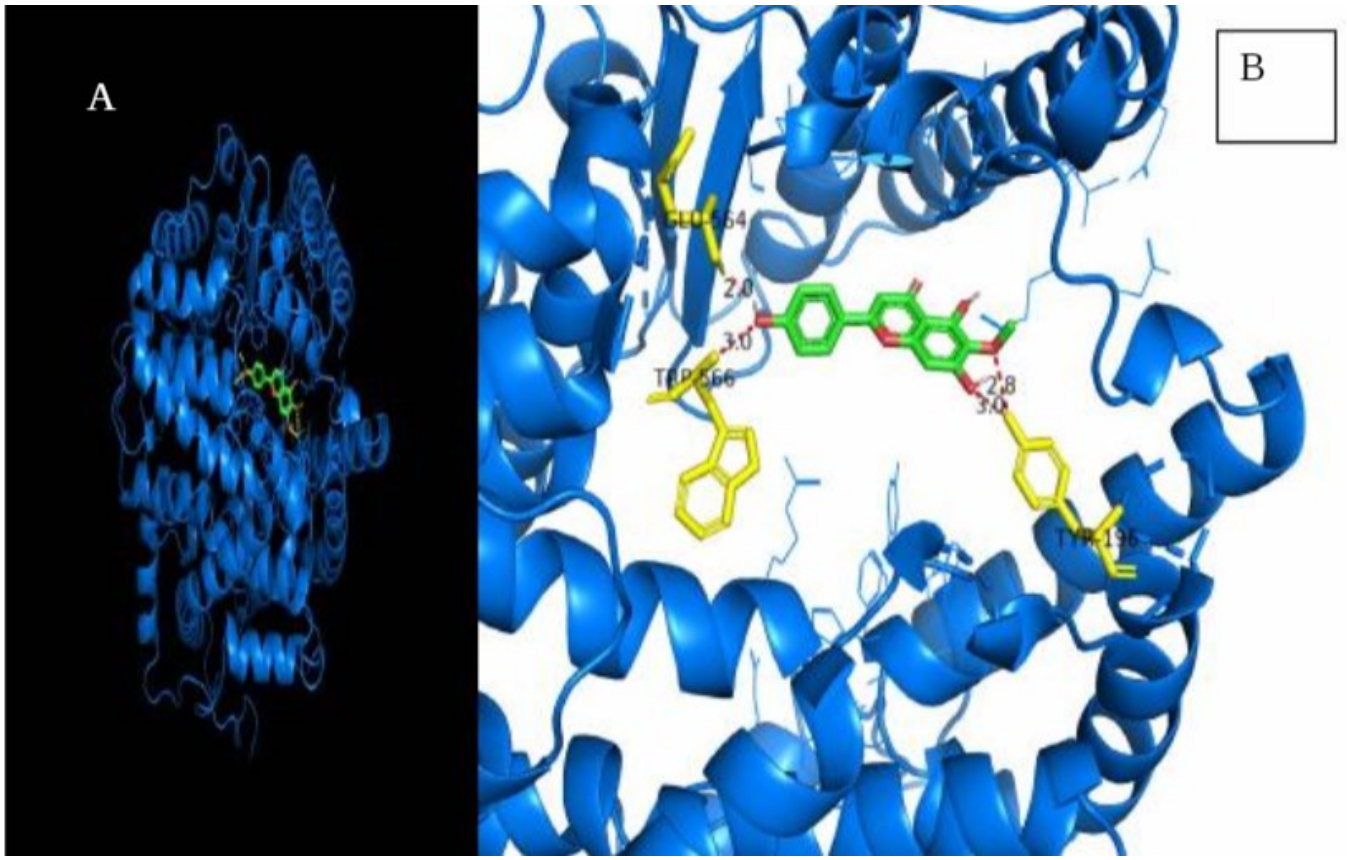

Figure9. Representation of docked ligand-protein complex (A) animation pose of Hispidulin within the cavity of ACE2, (B) Interaction of Hispidulin with amino acid residues of ACE2.

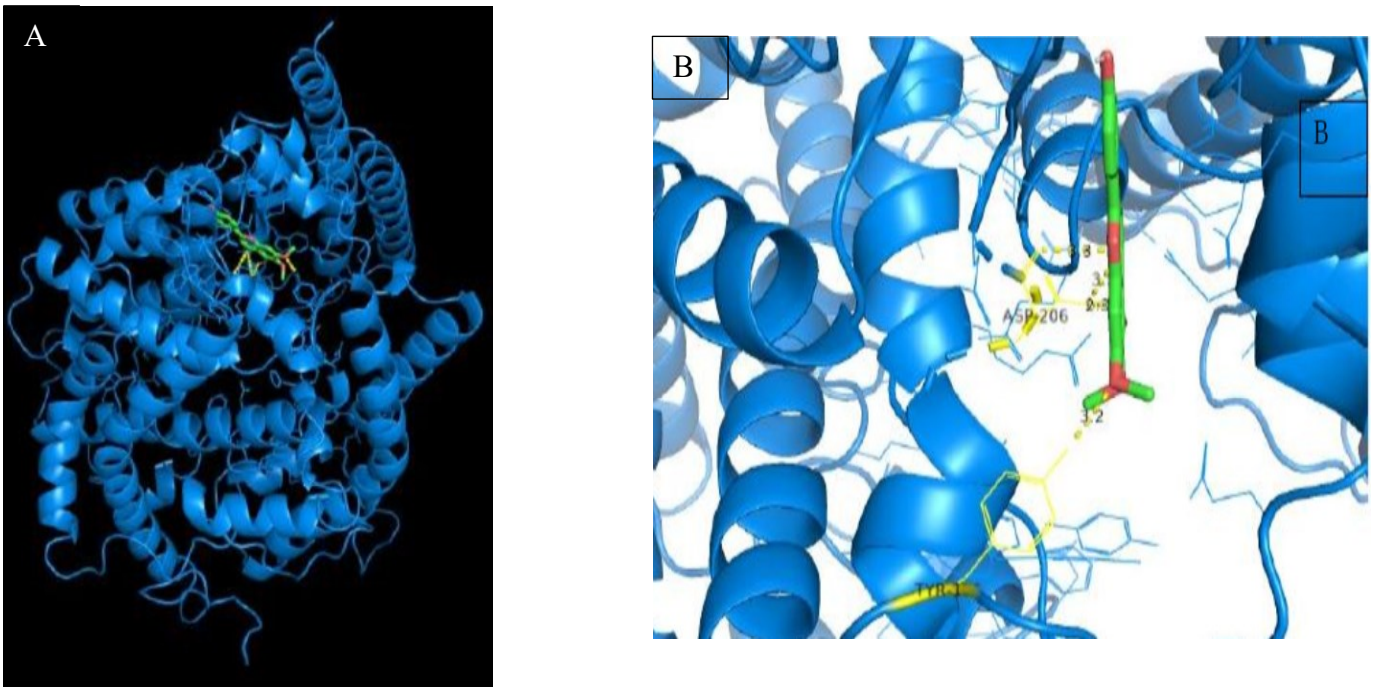

Figure 10. Representation of docked ligand-protein complex (A) animation pose of Cirsimaritin within the cavity of ACE2, (B) Interaction of Cirsimaritin with amino acid residues of ACE2.

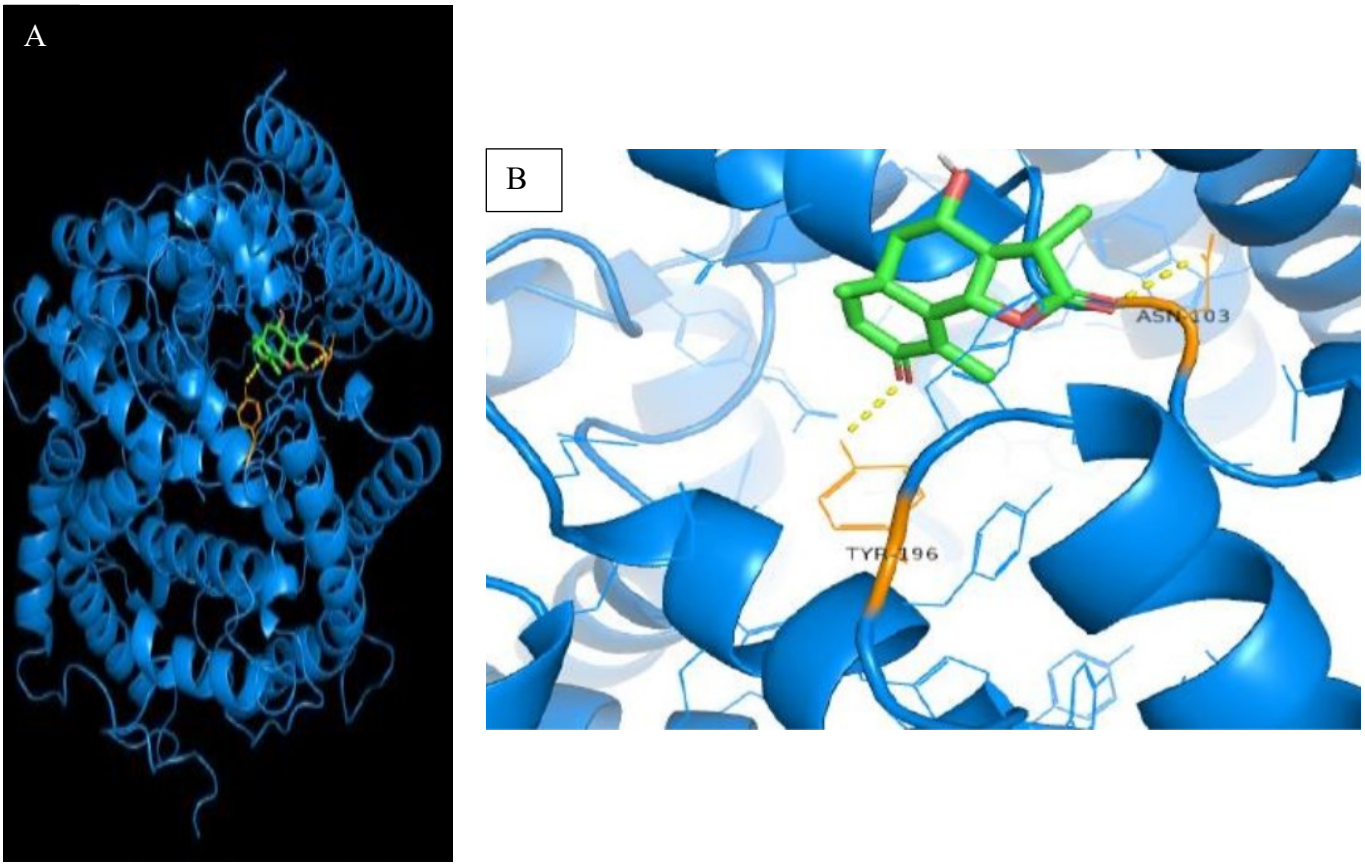

Figure 11. Representation of docked ligand-protein complex (A) animation pose of Artemisin within the cavity of ACE2, (B) Interaction of Artemisin with amino acid residues of ACE2.

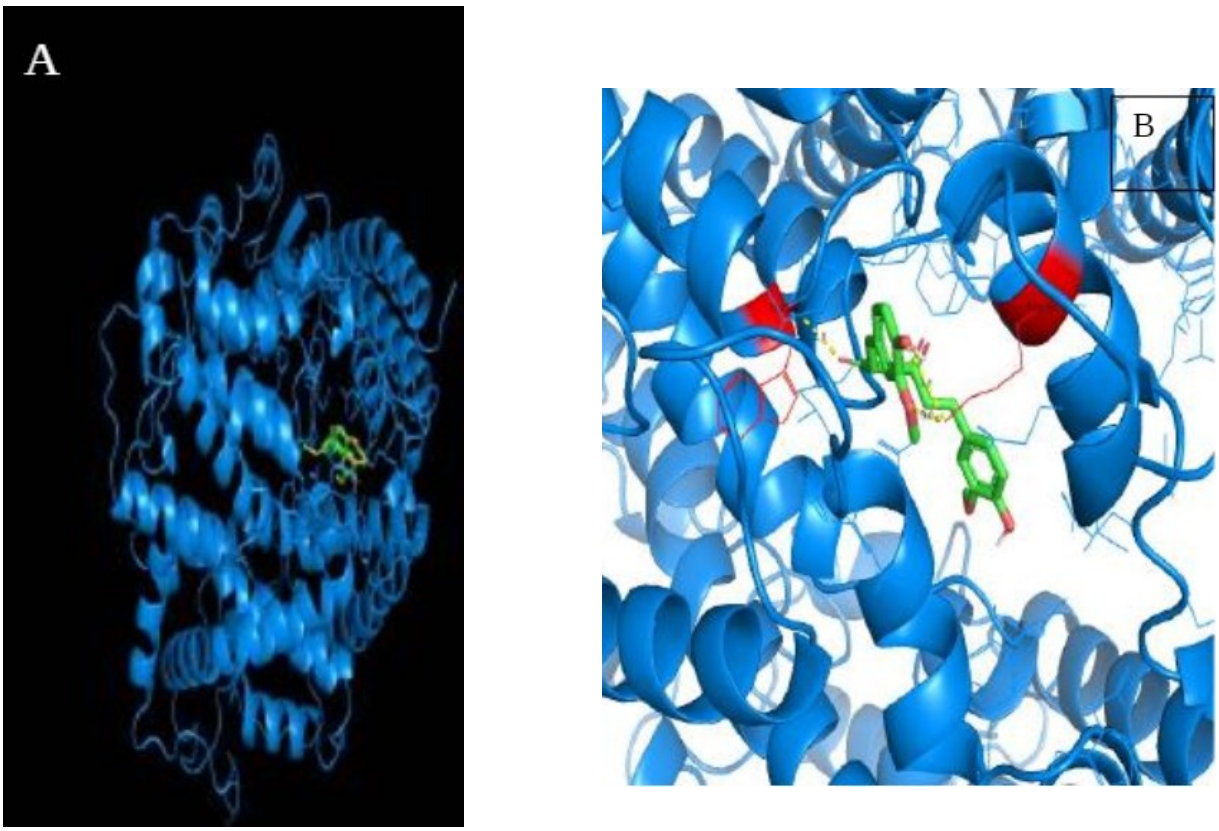

Figure 12. Representation of docked ligand-protein complex (A) animation pose of Curcuma within the cavity of ACE2, (B) Interaction of Curcuma with amino acid residues of ACE2.

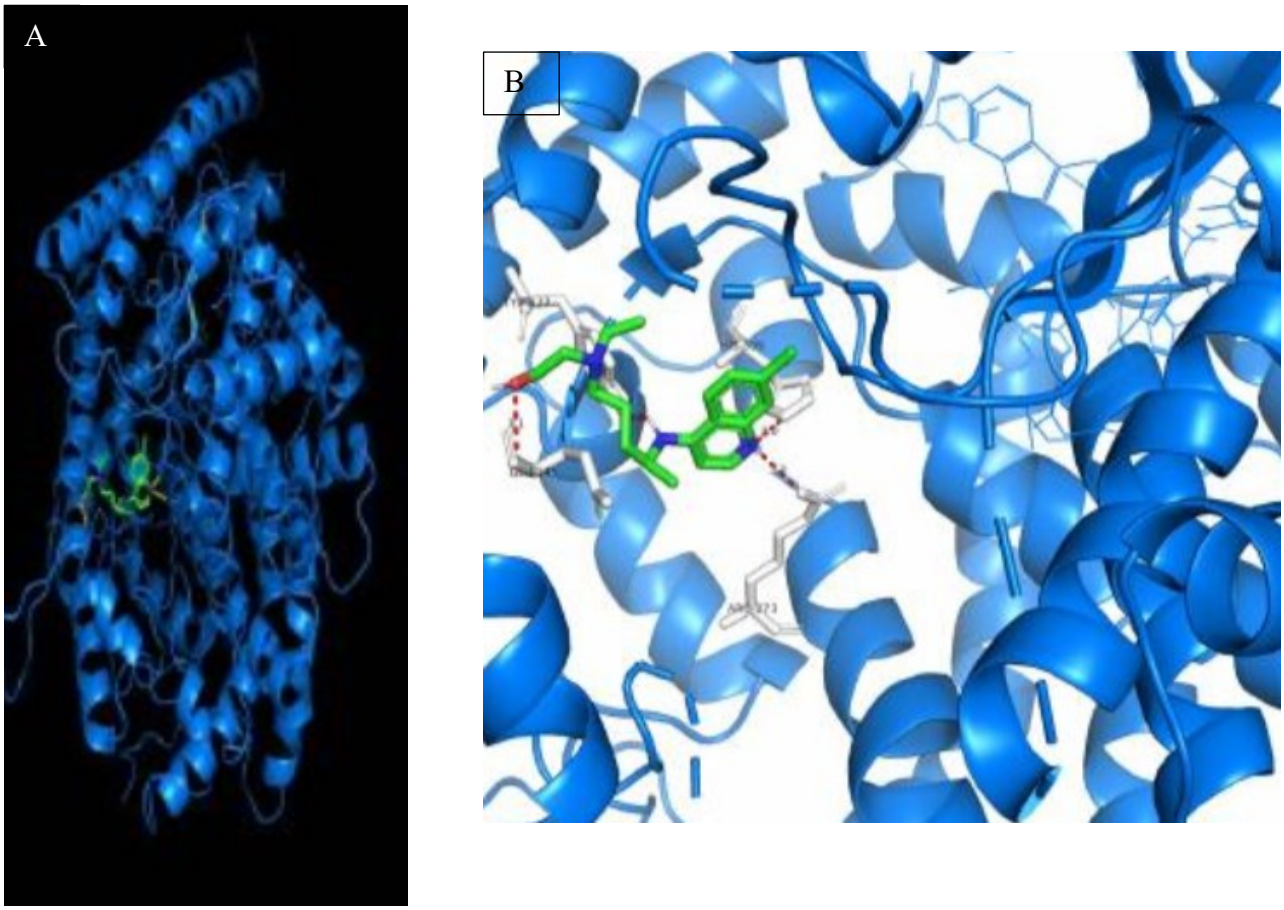

Figure 13. Representation of docked ligand-protein complex (A) animation pose of Hydroxychloroquine within the cavity of ACE2, (B) Interaction of Hydroxychloroquine with amino acid residues of ACE2.

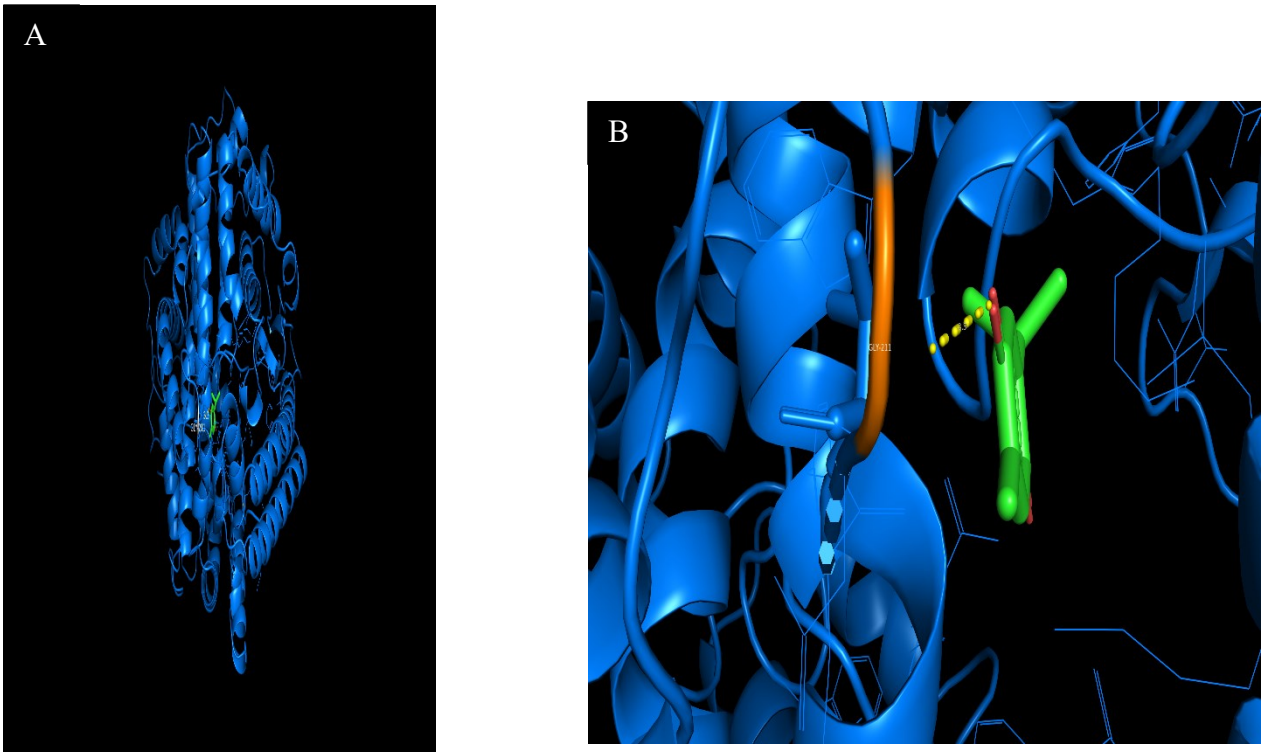

Figure 14. Representation of docked ligand-protein complex (A) animation pose of Thymoquinone within the cavity of ACE2, (B) Interaction of Thymoquinone with amino acid residues of ACE2.

5. Discussions

According to *in silico* results, Quercetin, Hispidulin, Cirsimaritin, Sulfasalazine, Artemisin, and Curcuma have a better affinity against COVİD 19 protease and ACE2 receptor better than Hydroxy-Chloroquine. The obtained results show also that Quercetin, Hispidulin, Cirsimaritin and Sulfasalazine exhibited as the best potential inhibitors against protease of COVID-19 and ACE2. Quercetin is an anti-oxidative flavonoid widely distributed in the plant kingdom, is a dietary antioxidant that prevents oxidation of low-density lipoproteins in vitro (Hollman et al.,1995). Quercetin is a flavonoid with a wide range of biological activities, is used in many countries as vasoprotectants (Erlund et al., 2000). Intake of quercetin was inversely associated with coronary heart disease mortality in elderly men (Murakami et al.,2008). Quercetin displays a large variety of biological activities including anticancer activity (Murakami et al.,2008), cardioprotective (Li et al., 2013), antioxidant and antidiabetic effect (Abdelmoaty et al., 2010). The protective effect of quercetin on chloroquine-induced oxidative stress and hepatotoxicity in mice was also approved (Kumar et al., 2013). According to in silico results, Quercetin have a better affinity against COVİD-19 protease better than Hydroxy-Chloroquine. The obtained results show also that Quercetin exhibited as the best potential inhibitors against protease of COVID-19.

Hispidulin, Cirsimaritin, and Artemisin are the main flavonoids isolated from Artemesia herba alba (Shen et al., 1994). Artemesia herba alba displays a large variety of biological activities including antidiabetic, antihyperlipidemic and nephroprotective (Sekiou et al., 2020, Sekiou et al., 2019), cardioprotective (Irshaid et al.,2012), anticancer (Khlifi et al.,2013), antioxidant (Sekiou et al., 2019), antiprotozoal (Bachrouch et al., 2015), gastroprotective (LAOUFI et LADJ, 2017), antibacterial (Yashphe et al., 1987), antihepatotoxic (Sekiou et al., 2019), insecticidal (Sharifian et al., 2012), Essential oils of Artemesia herba alba have also antihypertensive activities (Zeggwagh et al., 2008). Sulfasalazine [Salazopyrin®] is an intestinal anti-inflammatory, developed in the 1950s to treat rheumatoid arthritis (Taffet et al., 1983). According to in silico results, Sulfasalazine have a better affinity against COVİD-19 protease better than Hydroxy-Chloroquine. The obtained results show also that Sulfasalazine exhibited as the best potential inhibitors against protease of COVID-19. Curcuma displays a large variety of biological activities including cardioprotective (El-Sayed et al.,2011), anticancer (Chaithongyot et al.,2015), antiprotozoal (Shahiduzzaman et al., 2009), antibacterial (Kim et al., 2008), antihepatotoxic (Kiso et al., 1983), insecticidal (de Souza et al., 2016), The effect of curcuma in experimental malaria has been also demonstrated by Gomes et al., (2018). According to in silico results, Curcuma have a better affinity against COVİD 19 protease and ACE2 receptor better than Hydroxy-Chloroquine. The obtained results show also that Curcuma exhibited as the best potential inhibitors against protease of COVID-19 and ACE2. Thymoquinone (TQ) is one of the bioactive component derived from the medicinal plant Nigella sativa. Thymoquinone (TQ) exhibited many biological effects including antihistaminic effect (Kanter et al.,2006), anti-asthmatic (GONCA et KURT, 2015). cardioprotective (GONCA et al.,2015), anticancer (Paramasivam et al.,2012), antibacterial (Halawani, 2009), antihepatotoxic (Daba et Abdel-Rahmann 1998), The effect of Thymoquinone in experimental malaria has been also

demonstrated by El-Sayed et al., (2019). According to in silico results, Thymoquinone have a good affinity against COVİD 19 protease and ACE2 receptor but its lower than Hydroxy-Chloroquine. The obtained results show also that Thymoquinone exhibited as the best potential inhibitors against protease of COVID-19 and ACE2. Eugenol an aromatic product frequently found in diversified herbal plants. Among these plant sources, clove and cinnamon are considered as the prosperous provenances of eugenol. eugenol exhibited many biological effects including anti-asthmatic effect (Pan et Dong, 2015). anticancer (Vidhya et Devaraj, 2011), antibacterial (Kollanoor et al.,2010), antihepatotoxic (Binu et al., 2018), Eugenol exhibited also a biological effect **against** malaria (Govindarajan et al., 2016). According to in silico results, Eugenol have a good affinity against COVİD 19 protease and ACE2 receptor but its lower than Hydroxy-Chloroquine. The obtained results show also that Eugenol exhibited as the best potential inhibitors against protease of COVID-19 and ACE2. N-acetyl cysteine (NAC), a synthetic derivative of cysteine, is a non-essential amino acid synthesized in the body from methionine. NAC is a sensor of reactive oxygen species, but its main role as a stem from its role as a precursor of cysteine, a limiting step in the synthesis of glutathione (Sevgiler et al., 2007). It can be administered orally or by intravenous infusion and can also be inhaled using a nebulizer (Dodd et al., 2008). N-acetylcysteine (NAC) is prescribed for chronic bronchitis. Its ability to thin the secretions of the bronchi (mucolytic action) could facilitate their elimination and improve the breathing of people suffering of chronic obstructive pulmonary diseases (COPD) (LU et ZHENG, 2013). By improving oxygenation and by restoring the intracellular reserves of GSH in activated granulocytes, NAC also reduces the syndrome of experimental and clinical acute respiratory distress (Laurent et al., 1996). Khaledifar et al., 2015 shows that NAC may increase the effects of angiotensin converting enzyme (ACE) inhibitor drugs. NAC may exert its antihypertensive effects directly or through its storage form, glutathione, by decreasing oxidative stress, and modulating levels of nitric oxide and other vasoactive molecules (Vasdev et al., 2009) . Another potential therapeutic application for NAC comes from its anti-inflammatory activity. The transcription factor NF-κB plays an essential role in many aspects of the inflammation cascade and the immune response by regulating the expression of related genes (Yamamoto & Gaynor, 2001). NAC is used to reconstitute GSH that has been used up (Dröge & Breitkreutz, 1999). Studies show that NAC blocks cytokine-stimulated HIV replication in an infected T-cell line, blocks viral production in monocyte cell lines, inhibits stimulated expression of HIV in lymphocyte and cell lines chronically infected T cells, inhibits NF-κB activation leading to inhibition of stimulated viral transcription and replication and slows the transition from latency to later stages of AIDS in people infected with HIV (Treitinger et al., 2004). According to in silico results, N-acetylcysteine have a good affinity against COVİD 19 protease and ACE2 receptor but its lower than Hydroxy-Chloroquine. The obtained results show also that N-acetylcysteine exhibited as the best potential inhibitors against protease of COVID-19 and ACE2. Camphor is a solid bicyclic organic compound derived from the camphor tree, a tree scientifically known as *Cinnamomum camphora*. Camphor was used to fight the cholera epidemic in 1831–32 (Millot 1837) and then against the Asian flu in 1957–58 (Setzer, 2016). Camphor exhibited also a biological effect against malaria (Ho et al., 2016). According to in silico results, Camphor have a good affinity

against COVİD 19 protease and ACE2 receptor but its lower than Hydroxy-Chloroquine. The obtained results show also that Camphor exhibited as the best potential inhibitors against protease of COVID-19 and ACE2.

6. Conclusion

Spreading outbreak of COVID-19 has challenged the healthcare sector of the world in the last few months. To contribute to this fight against COVID-19, virtual screening based molecular docking was performed to identify novel compounds having the potential to bind Mpro of COVID-19 and ACE2. Our results demonstrate that Quercetin, Hispidulin, Cirsimaritin, Sulfasalazine, Artemisin, and Curcuma have a better binding affinity to Mpro of COVID-19 protease and ACE2 receptor better than Hydroxy-Chloroquine. Those molecules can be used as therapeutics against COVID-19. However, further studies should be conducted for the validation of these compounds using in vitro and in vivo models to pave a way for these compounds in drug discovery.

Acknowledgment

The present work was supported by DG-RSDT (General Directorate of Scientific Research and Technological Development-Algeria) via the Environmental Research Center (C.R.E), Campus, Sidi Amar, Annaba 23001; Algeria

.

Disclosure Statement

The authors report no conflict of interest.

Reference

Abdelmoaty, M. A., Ibrahim, M. A., Ahmed, N. S., & Abdelaziz, M. A. (2010). Confirmatory studies on the antioxidant and antidiabetic effect of quercetin in rats. *Indian Journal of Clinical Biochemistry*, *25*(2), 188-192.

Bachrouch, O., Ferjani, N., Haouel, S., & Jemâa, J. M. B. (2015). Major compounds and insecticidal activities of two Tunisian Artemisia essential oils toward two major coleopteran pests. Industrial Crops and Products, 65, 127-133.

Belouzard, Sandrine, MILLET, Jean K., LICITRA, Beth N., *et al.* Mechanisms of coronavirus cell entry mediated by the viral spike protein. *Viruses*, 2012, vol. 4, no 6, p. 1011-1033.

Binu, P., Nellikunnath Priya, M. P. H. I. L., Abhilash, S., Vineetha, R. C., & Nair, H. (2018). Protective effects of eugenol against hepatotoxicity induced by arsenic trioxide: An antileukemic drug. *Iranian journal of medical sciences*, *43*(3), 305.

Chaithongyot, S., Asgar, A., Senawong, G., Yowapuy, A., Lattmann, E., Sattayasai, N., & Senawong, T. (2015). Anticancer effects of curcuma C20-dialdehyde against colon and cervical cancer cell lines. *Asian Pacific Journal of Cancer Prevention*, *16*(15), 6513-6519.

Daba, M. H., & Abdel-Rahman, M. S. (1998). Hepatoprotective activity of thymoquinone in isolated rat hepatocytes. *Toxicology letters*, *95*(1), 23-29.

de Souza Tavares, W., Akhtar, Y., Gonçalves, G. L. P., Zanuncio, J. C., & Isman, M. B. (2016). Turmeric powder and its derivatives from Curcuma longa rhizomes: insecticidal effects on cabbage looper and the role of synergists. *Scientific reports*, *6*, 34093.

DODD, Seetal, DEAN, Olivia, COPOLOV, David L., *et al.* N-acetylcysteine for antioxidant therapy: pharmacology and clinical utility. *Expert opinion on biological therapy*, 2008, vol. 8, no 12, p. 1955-1962.

DRÖGE, Wulf et BREITKREUTZ, Raoul. N-acetyl-cysteine in the therapy of HIV-positive patients. *Current Opinion in Clinical Nutrition & Metabolic Care*, 1999, vol. 2, no 6, p. 493-498.

El-Sayed, E. M., El-azeem, A. S., Afify, A. A., Shabana, M. H., & Ahmed, H. H. (2011). Cardioprotective effects of Curcuma longa L. extracts against doxorubicin-induced cardiotoxicity in rats. *J Med Plants Res*, *5*(17), 4049-4058.

El-Sayed, S. A. E. S., Rizk, M. A., Yokoyama, N., & Igarashi, I. (2019). Evaluation of the in vitro and in vivo inhibitory effect of thymoquinone on piroplasm parasites. *Parasites & vectors*, *12*(1), 37.

Erlund, I., Kosonen, T., Alfthan, G., Mäenpää, J., Perttunen, K., Kenraali, J., ... & Aro, A. (2000). Pharmacokinetics of quercetin from quercetin aglycone and rutin in healthy volunteers. European journal of clinical pharmacology, 56(8), 545-553.

Gomes, G. S., Maciel, T. R., Piegas, E. M., Michels, L. R., Colomé, L. M., Freddo, R. J., ... & Haas, S. E. (2018). Optimization of curcuma oil/quinine-loaded nanocapsules for malaria treatment. *AAPS PharmSciTech*, *19*(2), 551-564.

GONCA, E., & KURT, Ç. (2015). Cardioprotective effect of Thymoquinone: A constituent of Nigella sativa L., against myocardial ischemia/reperfusion injury and ventricular arrhythmias in anaesthetized rats. *Pakistan Journal of Pharmaceutical Sciences*, *28*(4).

Govindarajan, M., Rajeswary, M., Hoti, S. L., Bhattacharyya, A., & Benelli, G. (2016). Eugenol, α-pinene and β-caryophyllene from Plectranthus barbatus essential oil as eco-friendly larvicides against malaria, dengue and Japanese encephalitis mosquito vectors. *Parasitology research*, *115*(2), 807-815.

Halawani, E. (2009). Antibacterial activity of thymoquinone and thymohydroquinone of Nigella sativa L. and their interaction with some antibiotics. *Advances in Biological Research*, *3*(5-6), 148-152.

Ho, D. D., Lau, C. P., Ng, K. H., Kong, Y. C., Cheng, K. F., & Chan, K. P. (1991). Anti-implantation activity of S (−)-and R (+)-camphor-yuehchukene in rats. *European journal of pharmacology*, *205*(2), 209-212.

Hollman, P. C., de Vries, J. H., van Leeuwen, S. D., Mengelers, M. J., & Katan, M. B. (1995). absorption of dietary quercetin glycosides and quercetin in healthy ileostomy volunteers. The American journal of clinical nutrition, 62(6), 1276-1282.

Irshaid, F., Mansi, K., Bani-Khaled, A., & Aburjia, T. (2012). Hepatoprotetive, cardioprotective and nephroprotective actions of essential oil extract of Artemisia sieberi in alloxan induced diabetic rats. Iranian journal of pharmaceutical research: IJPR, 11(4), 1227.

Kanter, M., Coskun, O., & Uysal, H. (2006). The antioxidative and antihistaminic effect of Nigella sativa and its major constituent, thymoquinone on ethanol-induced gastric mucosal damage. *Archives of toxicology*, *80*(4), 217-224.

Keyhanmanesh, R., Boskabady, M. H., Khamneh, S., & Doostar, Y. (2010). Effect of thymoquinone on the lung pathology and cytokine levels of ovalbumin-sensitized guinea pigs. *Pharmacological reports*, *62*(5), 910-916.

KHALEDIFAR, Arsalan, MOBASHERI, Mahmoud, KHEIRI, Soleiman, *et al.* Comparison of N-acetylcysteine and angiotensin converting enzyme inhibitors in blood pressure regulation in hypertensive patients. *ARYA atherosclerosis*, 2015, vol. 11, no 1, p. 5.

Khlifi, D., Sghaier, R. M., Amouri, S., Laouini, D., Hamdi, M., & Bouajila, J. (2013). Composition and anti-oxidant, anti-cancer and anti-inflammatory activities of Artemisia herba-alba, Ruta chalpensis L. and Peganum harmala L. Food and chemical toxicology, 55, 202-208.

Kim, J. E., Kim, H. E., Hwang, J. K., Lee, H. J., Kwon, H. K., & Kim, B. I. (2008). Antibacterial characteristics of Curcuma xanthorrhiza extract on Streptococcus mutans biofilm. *The Journal of Microbiology*, *46*(2), 228.

Kiso, Y., Suzuki, Y., Watanabe, N., Oshima, Y., & Hikino, H. (1983). Antihepatotoxic principles of Curcuma longa rhizomes. *Planta medica*, *49*(11), 185-187.

Kitchen D, Decornez H, Furr J, Bajorath J. Docking and scoring in virtual screening for drug discovery: methods and applications. Nat Rev Drug Discov. 2004;3(11):935–949. doi: 10.1038/nrd1549).

Kollanoor Johny, A., Darre, M. J., Donoghue, A. M., Donoghue, D. J., & Venkitanarayanan, K. (2010). Antibacterial effect of trans-cinnamaldehyde, eugenol, carvacrol, and thymol on Salmonella Enteritidis and Campylobacter jejuni in chicken cecal contents in vitro. *Journal of Applied Poultry Research*, *19*(3), 237-244.

Kumar Mishra, S., Singh, P., & Rath, S. K. (2013). Protective effect of quercetin on chloroquine-induced oxidative stress and hepatotoxicity in mice. *Malaria research and treatment*, *2013*.

LAOUFI, T., & LADJ, M. (2017). *Artemisia herba-alba anti-inflammatory activity and gastro-protective effects in mice* (Doctoral dissertation, Université de Bouira).

LAURENT, Thierry, MARKERT, Michèle, FEIHL, Francois, *et al.* Oxidant-antioxidant balance in granulocytes during ARDS: Effect of N-acetylcysteine. *Chest*, 1996, vol. 109, no 1, p. 163-166.

Li, M., Jiang, Y., Jing, W., Sun, B., Miao, C., & Ren, L. (2013). Quercetin provides greater cardioprotective effect than its glycoside derivative rutin on isoproterenol-induced cardiac fibrosis in the rat. *Canadian journal of physiology and pharmacology*, *91*(11), 951-959.

LIU, Zhixin, XIAO, Xiao, WEI, Xiuli, *et al.* Composition and divergence of coronavirus spike proteins and host ACE2 receptors predict potential intermediate hosts of SARS-CoV-2. *Journal of medical virology*, 2020.

LU, Wenju et ZHENG, Jinping. The function of mucins in the COPD airway. *Current Respiratory Care Reports*, 2013, vol. 2, no 3, p. 155-166.

MCINTOSH, Kenneth et PERLMAN, Stanley. Coronaviruses, including severe acute respiratory syndrome (SARS) and Middle East respiratory syndrome (MERS). *Mandell, Douglas, and Bennett's Principles and Practice of Infectious Diseases, Updated Edition. 8th ed. Philadelphia, PA: Elsevier Saunders*, 2015.

Millot, D. B. J. L. (1837). *Histoire pharmacologique du camphre...* GG Levrault.

Murakami, A., Ashida, H., & Terao, J. (2008). Multitargeted cancer prevention by quercetin. Cancer letters, 269(2), 315-325.

Oleg Trott and Arthur J. Olson AutoDock Vina: improving the speed and accuracy of docking with a new scoring function, efficient optimization and multithreading.J Comput Chem. 2010 Jan 30; 31(2): 455–461. doi: 10.1002/jcc.21334

Pan, C., & Dong, Z. (2015). Antiasthmatic effects of eugenol in a mouse model of allergic asthma by regulation of vitamin D3 upregulated protein 1/NF-κB pathway. *Inflammation*, *38*(4), 1385-1393.

Paramasivam, A., Sambantham, S., Shabnam, J., Raghunandhakumar, S., Anandan, B., Rajiv, R., ... & Jayaraman, G. (2012). Anti-cancer effects of thymoquinone in mouse neuroblastoma (Neuro-2a) cells through caspase-3 activation with down-regulation of XIAP. *Toxicology letters*, *213*(2), 151-159.

ROBSON, B. Computers and viral diseases. Preliminary bioinformatics studies on the design of a synthetic vaccine and a preventative peptidomimetic antagonist against the SARS-CoV-2 (2019-nCoV, COVID-19) coronavirus. *Computers in Biology and Medicine*, 2020, p. 103670.

Sekiou, O., Boumendjel, M., Taibi, F., Boumendjel, A., & Messarah, M. (2019). Mitigating effects of antioxidant properties of Artemisia herba alba aqueous extract on hyperlipidemia and oxidative damage in alloxan-induced diabetic rats. Archives of physiology and biochemistry, 125(2), 163-173.

Sekiou, O., Boumendjel, M., Taibi, F., Tichati, L., Boumendjel, A., & Messarah, M. (2020). Nephroprotective effect of Artemisia herba alba aqueous extract in alloxan-induced diabetic rats. Journal of Traditional and Complementary Medicine.

Setzer, W. N. (2016). Essential oils as complementary and alternative medicines for the treatment of influenza. *American Journal of Essential Oils and Natural Products*, *4*(4), 16-22.

SEVGILER, Y., PINER, P., DURMAZ, H., *et al.* Effects of N-acetylcysteine on oxidative responses in the liver of fenthion exposed Cyprinus carpio. *Pesticide biochemistry and physiology*, 2007, vol. 87, no 3, p. 248-254.

Shahiduzzaman, M., Dyachenko, V., Khalafalla, R. E., Desouky, A. Y., & Daugschies, A. (2009). Effects of curcumin on Cryptosporidium parvum in vitro. *Parasitology research*, *105*(4), 1155-1161.

Sharifian, I., Hashemi, S. M., Aghaei, M., & Alizadeh, M. (2012). Insecticidal activity of essential oil of Artemisia herba-alba Asso against three stored product beetles. *Biharean Biologist*, *6*(2), 90-93.

Shen, X. L., Nielsen, M., Witt, M. R., Sterner, O., Bergendorff, O., & Khayyal, M. O. H. A. M. E. D. (1994). Inhibition of [methyl-3H] diazepam binding to rat brain membranes in vitro by dinatin and skrofulein. Zhongguo yao li xue bao= Acta pharmacologica Sinica, 15(5), 385-388.

SU, Shuo, WONG, Gary, SHI, Weifeng, *et al.* Epidemiology, genetic recombination, and pathogenesis of coronaviruses. *Trends in microbiology*, 2016, vol. 24, no 6, p. 490-502.

Taffet, S. L., & Das, K. M. (1983). Sulfasalazine. *Digestive diseases and sciences*, *28*(9), 833-842.

TREITINGER, Aricio, SPADA, Celso, MASOKAWA, Ivete Yoshico, *et al.* Effect of N-acetyl-L-cysteine on lymphocyte apoptosis, lymphocyte viability, TNF-alpha and IL-8 in HIV-infected patients undergoing anti-retroviral treatment. *Brazilian Journal of Infectious Diseases*, 2004, vol. 8, no 5, p. 363-371.

VASDEV, Sudesh, SINGAL, Pawan, et GILL, Vicki. The antihypertensive effect of cysteine. *International Journal of Angiology*, 2009, vol. 18, no 01, p. 07-21.

Vidhya, N., & Devaraj, S. N. (2011). Induction of apoptosis by eugenol in human breast cancer cells.

YAMAMOTO, Yumi et GAYNOR, Richard B. Role of the NF-kB pathway in the pathogenesis of human disease states. *Current molecular medicine*, 2001, vol. 1, no 3, p. 287-296

Yashphe, J., Feuerstein, I., Barel, S., & Segal, R. (1987). The antibacterial and antispasmodic activity of Artemisia herba alba Asso. II. Examination of essential oils from various chemotypes. *International journal of crude drug research*, *25*(2), 89-96.

Zeggwagh, N. A., Farid, O., Michel, J. B., & Eddouks, M. (2008). Cardiovascular effect of Artemisia herba alba aqueous extract in spontaneously hypertensive rats. *Methods and findings in experimental and clinical pharmacology*, *30*(5), 375-381.

Zhou Y., Hou Y., Shen J., Huang Y., Martin W., Cheng F. (2020) Network-based drug repurposing for novel oronavirus 2019-nCoV/SARS-CoV-2. Cell Discovery. 6.